Pathology of Berkeley sickle cell mice: similarities and differences with human sickle cell disease

Elizabeth A. Manci, Cheryl A. Hillery, Carol A. Bodian, Zheng G. Zhang, Gerard A. Lutty, and Barry S. Coller

Because Berkeley sickle cell mice are used as an animal model for human sickle cell disease, we investigated the progression of the histopathology in these animals over 6 months and compared these findings to those published in humans with sickle cell disease. The murine study groups were composed of wild-type mixed C57Bl/6-SV129 (control) mice and sickle cell (SS) mice ($\alpha^{-/-}$, $\beta^{-/-}$, transgene +) of both sexes and between 1 and 6 months of age. SS mice were similar to humans with sickle cell disease in having erythrocytic sickling, vascular ectasia, intravascular hemolysis, exuberant hematopoiesis, cardiomegaly, glomerulosclerosis, visceral congestion, hemorrhages, multiorgan infarcts, pyknotic neurons, and progressive siderosis. Cerebral perfusion studies demonstrated increased blood-brain barrier permeability in SS mice. SS mice differed from humans with sickle cell disease in having splenomegaly, splenic hematopoiesis, more severe hepatic infarcts, less severe pulmonary manifestations, no significant vascular intimal hyperplasia, and only a trend toward vascular medial hypertrophy. Early retinal degeneration caused by a homozygous mutation (rd1) independent from that causing sickle hemoglobin was an incidental finding in some Berkeley mice. While our study reinforces the fundamental strength of this model, the notable differences warrant careful consideration when drawing parallels to human sickle cell disease. (Blood. 2006;107: 1651-1658)

Introduction

Several murine models have been developed to mimic human sickle cell (SS) disease. Of these, the Berkeley SS model has targeted deletions of murine α and β globins ($\alpha^{-/-}$, $\beta^{-/-}$) with a transgene containing human α, β^s, $^A\gamma$, $^G\gamma$, and β globins; thus, these mice express human sickle hemoglobin almost exclusively.[1,2] Berkeley SS mice have several hematologic as well as histopathologic similarities and differences compared with human sickle cell disease. Published similarities include erythrocytic sickling, intravascular hemolysis, reticulocytosis, severe anemia (hematocrit, 10%-30%), leukocytosis, elevations of inflammatory cytokines, defects in urine concentrating ability, multiorgan infarcts, glomerulosclerosis, and pulmonary congestion.[1-5] Published differences include lower-than-normal mean corpuscular hemoglobin concentrations, suggesting a partial thalassemic phenotype, and splenomegaly with exuberant splenic hematopoiesis in SS mice, rather than the higher-than-normal mean corpuscular hemoglobin concentrations and progressive splenic infarcts and atrophy with exuberant bone marrow hematopoiesis typical of human sickle cell disease.[2] In addition, the erythrocytes of Berkeley SS mice, like those of all murine strains, have red-cell volumes that are considerably smaller than those of human erythrocytes.

Relatively little attention has been given to comparison of the natural progression of chronic organ injury in this model with that in human sickle cell disease. Potential strengths of murine models of sickle cell disease include the ability to intervene therapeutically and to crossbreed the mice with other mice harboring targeted genetic alterations for assessment of the impact of the therapeutic interventions and/or genetic alterations on the hematologic abnormalities and chronic organ injury in the SS mice. To achieve these goals, however, it is necessary to have a detailed understanding of the rate of development and severity of visceral pathology in SS mice, stratified for sex and age. This study was initiated to improve our understanding of the natural progression of organ pathology in Berkeley SS mice for both comparison with human sickle cell disease and as a baseline for assessing the effects of therapeutic interventions and/or genetic alterations.

Materials and methods

Transgenic and control mice

The Berkeley sickle mice with genotype Tg(Hu-miniLCR α1 $^G\gamma$ $^A\gamma\delta$ β^s) *Hba*^{0} *Hba*^{0} *Hbb*^{0} *Hbb*^{0} and the hemizygous mice with genotype Tg(Hu-miniLCR α1 $^G\gamma$ $^A\gamma$ δ β^s) *Hba*^{0} *Hba*^{0} *Hbb*^{0} *Hbb*$^+$ were littermates of similar

From The Department of Pathology, Centralized Pathology Unit for Sickle Cell Disease, University of South Alabama, Mobile; the Medical College of Wisconsin and The Blood Center of Southeastern Wisconsin, Milwaukee; the Department of Anesthesiology, Mount Sinai School of Medicine, New York, NY; the Department of Neurology, Henry Ford Hospital, Detroit, MI; the Wilmer Ophthalmological Institute, Johns Hopkins Hospital, Baltimore, MD; and the Laboratory of Blood and Vascular Biology, The Rockefeller University, New York, NY.

Submitted July 21, 2005; accepted August 26, 2005. Prepublished online as *Blood* First Edition Paper, September 15, 2005; DOI 10.1182/blood-2005-07-2839.

Supported in part by contract N01-HB-07086 (E.A.M.); grants HL44612 (C.A.H.), HL70981 (C.A.H.), HL45922 (G.A.L.), and HL19278 (B.S.C.) from the National Heart, Lung and Blood Institute; NS43324 from the National Institute of Neurological Disorders and Stroke; and funds from Stony Brook University.

Presented in part in abstract form at the 45th annual meeting of the American Society of Hematology, San Diego, CA, December 6, 2003.

Reprints: Elizabeth Manci, Children's and Women's Hospital Laboratory, 1700 Center St, Mobile, AL 36604; e-mail: emanci@usouthal.edu.

The publication costs of this article were defrayed in part by page charge payment. Therefore, and solely to indicate this fact, this article is hereby marked "advertisement" in accordance with 18 U.S.C. section 1734.

Table 1. Organ weights as actual weights and as percentages of body weights in control and sickle mice

	Mean or percentage		*P*		
	SS; n = 14	WT; n = 10	Sickle vs WT	Male vs female	Increasing age
Age, mo	3.5	3.4	.84	NA	NA
Body weight, g	21.0	23.2	.23	NA	NA
Male, % of total	50	50	> .99	NA	NA
Actual organ weight, g					
Spleen	1.2	0.11	< .001*	.26*	.01*
Heart	0.18	0.14	.02*	.02*	.02*
Brain	0.41	0.37	.03*	.77*	.04*
Liver	1.5	1.4	.28*	< .001*	< .001*
Kidneys	0.40	0.37	.42*	< .001*	< .001*
Body weight, % of total					
Spleen	5.7	0.47	NA	NA	NA
Heart	0.85	0.63	NA	NA	NA
Brain	2.0	1.7	NA	NA	NA
Liver	6.9	5.8	NA	NA	NA
Kidneys	1.9	1.6	NA	NA	NA

NA indicates not applicable.
**P* values for multiple regression with 3 factors.

background. All of the hemizygous mice carried one transgene. These mice were supplied by Dr Mohandas Narla of The New York Blood Center and were housed and bred at the Medical College of Wisconsin Animal Resource Center. Control mice, interbred progeny of a cross between C57Bl/6 and 129S mice (2 of the 5 parental strains of the Berkeley mice), were housed and bred at Rockefeller University. Age and sex distributions by genotype for the mice studied for organ weights are detailed in Table 1 and those for histopathology in Table 2.

Ten of the control mice used for organ weights also were studied for histopathology.

Hematologic parameters

After administering anesthesia (Avertin, ~0.5 mg/gm body weight), phlebotomy was performed on 16 SS mice (age, 2-14 months; mean, 6.5 months) of both sexes via the retro-orbital venous plexus or the left ventricle. Blood was collected into heparinized saline (4%-5% dilutional effects), and then the hematocrit (hct), mean red-cell volume (MCV), and mean red-cell hemoglobin concentration (MCHC) were determined using an automated veterinary blood counter (Heska; Fort Collins, CO). The reticulocyte count was determined by flow cytometry using thiazole orange, based on the percentage of thiazole orange–positive cells within the erythrocyte gate.

Organ weights

Control and SS mice were weighed, anesthetized, euthanized, and sent to the University of South Alabama for dissection. The spleen, liver, heart, kidneys, and brain were removed and weighed (Table 1). Organ weight data are reported as both actual measured weights and as percentages of body weight.

Histopathology

At specified ages, animals were weighed, anesthetized, and either prepared as indicated in "Organ weights" or perfusion-fixed with 10 mL phosphate-buffered saline (PBS) at 37°C, followed by 10 mL 4% paraformaldehyde in PBS. Perfusion was continued until clear fluid was obtained from the right atrium in all animals. The animals were partially dissected to expose intracranial, thoracic, and abdominal viscera; immersion-fixed in 4% paraformaldehyde (at least 7 days at 4°C); and sent to the University of South Alabama for dissection. Tissue was harvested by removal of the calvarium for extraction of the brain and brainstem, enucleation of the eyes, Rokitansky evisceration, and representative samplings of ribs, sternum, thoracolumbar vertebrae, and spinal cord. Tissues sampled for microscopic studies included skeletal muscle, cerebral hemispheres, brainstem, cerebellum, eyes, thymus, lungs, heart, spleen, liver, pancreas, kidneys, adrenals, stomach, small and large intestines, and bone with marrow from ribs and vertebrae. The animals were then sent to the Henry Ford Hospital (Detroit, MI), where the internal carotids of 2 control and 2 SS mice (both sexes, age 5 or 6 months old) were isolated under a surgical microscope and cross-sectioned (8 μm) for routine processing.

All 15 of the SS animals and 6 of the control animals analyzed for histopathology were perfusion-fixed. Organs from 10 control animals used for the weight study also were included for some parts of the histopathology study after determining that the method of preparation did not affect the results. These animals were not included in analyses judged potentially to be affected by the perfusion fixation (perivenous pallor in the liver, intravascular sickling, and pulmonary capillary congestion and hemorrhage) or affected by delayed fixation (microscopic acute hepatic infarcts and estimation of splenic hematopoiesis).

Tissues were embedded in paraffin, sectioned at 5 to 7 microns, and stained with hematoxylin and eosin (H&E). At least 3 sections per tissue block of viscera were stained with H&E for light microscopy. Additional sections were made for special stains, including Gomori modified Prussian blue stain for iron, Masson trichrome stain for fibrous connective tissue (infarcts) and degenerating neurons, and Verhoff–von Giesson stain for elastic fibers, each with appropriate controls. The murine microscopic studies were masked to age, sex, and genotype. Criteria for scoring of morphologic features are summarized in Table 3.

Measurements were made using an ocular micrometer at 40 × for islet diameter, glomerular size, renal cortical thickness, and vascular diameter, or a vernier caliper (mm) for spleen diameter. Mean micrometer measurements indicate the average of 10 randomly selected areas. Photomicrographs were made using a Zeiss Axioskop (Zeiss, Thornwood, NY) and formatted using Adobe Photoshop (Adobe Systems, San Jose, CA). The specific features selected for grading on H&E stains are summarized in Table 4.

Eyes from SS mice were either serially cross-sectioned or dissected so as to study the retina. For the latter, after removal of the vitreous, retinas were separated carefully from the retinal pigment epithelium and choroid and fixed in 2% paraformaldehyde in 0.1 M cacodylate buffer overnight at 4°C. Retinas were washed in 0.1 M cacodylate buffer with 5% sucrose and then analyzed for adenosine diphosphatase (ADPase) activity, a marker of viable blood vessels, by histochemistry, as previously published.[6]

After the ADPase incubation, retinas were opened with relaxing cuts and fixed flat in 25% Karnovsky fixative, pH 7.4, at 4°C overnight or longer. The tissue was then washed, dehydrated, and infiltrated and embedded in glycol methacrylate (JB-4, Polysciences; Warrington, PA), as published previously.[6] Using dark-field illumination, the blood vessels in the whole block were photographed and mapped. Sections (2.5 μm) were cut on a dry glass knife with a Sorvall NT2 microtome (Sorvall, Newtown, CT), and the sections were stained with periodic acid-Schiff and hematoxylin or thionin and ammonium sulfide to stain the cell nuclei blue and develop the ADPase activity.[6]

Cerebral vasculature

After isoflurane anesthesia, fluorescein isothiocyanate (FITC) dextran (2×10^6 molecular weight; Sigma, St Louis, MO; 0.1 mL of 25 mg/mL in

Table 2. Number of mice by genotype, sex, and age for histopathology studies

	Control		Sickle	
Age, mo	M	F	M	F
1	2	2	2	1
2	0	0	1	3
3	3	3	0	2
4	0	0	1	1
5	1	1	2	0
6	2	2	1	1

M indicates male; F, female.

Table 3. Scoring criteria for morphologic findings

Score	Degree	Distribution	Magnification	Field involved, %	Glomerular size, U
0	Absent	Normal	—	0	6
1	Minimal	1-2 cells	400 ×	10-30	7
2	Mild	Focal cluster	400 ×	30-50	8
3	Mild-moderate	Few clusters	100 ×	50	9
4	Moderate	Many clusters	100 ×	50-70	10
5	Moderate-severe	Every field	25 ×	70-90	11
6	Severe/abundant	Most cells	25 ×	90-100	12

— indicates not applicable.

saline) was administered intravenously via the saphenous vein to 1 control and 1 SS mouse to delineate the vascular tree as previously described. Five minutes later, the mice were euthanized and the brains rapidly removed and placed in 4% paraformaldehyde at 4°C for 72 hours, followed by storage in PBS at 4°C. Tissue was then sent to the Henry Ford Hospital, where coronal sections (100 μm) were cut on a vibratome and analyzed using a Bio-Rad MRC 1024 (argon and krypton) laser-scanning confocal imaging system mounted onto a Zeiss microscope (Bio-Rad; Cambridge, MA).[7] Areas of interest were scanned with a 10 ×/0.22 or 40 ×/1.0 oil-immersion objective lens in 512 × 512 pixel (1042 × 1042 μm for 10 × or 260.6 × 260.6 μm for 40 ×) format in the x-y direction using a 4 × frame-scan average.

DNA analysis for rd1 mutation

Genomic DNA was prepared from the tails of mice after digestion with Dd1 as described.[8] Primers to detect the rd1 mutation, which affects the rod photoreceptor cGMP phosphodiesterase, were employed and the mutation detected as previously described.[8]

Statistical analysis

Data for each feature were summarized for sickle cell and for control animals, and then the groups were compared. Means were calculated for variables measured on a continuous scale or on a grading scale with outcomes spread over a large part of the 0-to-6 range. These mean values were compared between groups by *t* tests. When most of the outcomes in either group equaled 0, outcomes with scores of 1 or greater were characterized as positive outcomes, and the proportions of each group with a positive outcome were compared using exact chi-square tests. Means of the positive values also were tabulated. As indicated by visual inspection of the data, effects of age and sex were sought by chi-square tests, Mantel-Haenszel tests, or linear regression analyses. The splenic white pulp was analyzed as measured, and also as proportional to the diameter of the spleen and to the square of the spleen diameter, as possible estimates of splenic volume, assuming that the spleen is approximately cylindrical.

Results

The hematologic data on the SS mice were similar to previously published data. Comparison of 16 SS mice with 5 controls showed severe anemia (hematocrit, 21% ± 7%; mean ± SD; controls, 42.1% ± 2.9%), reduced MCV and MCHC (42 ± 2 fl and 31 ± 2 fl, respectively; controls 46 ± 1 and 33.4 ± 0.4, respectively), and markedly elevated reticulocyte count (48% ± 8%; controls, 4.9% ± 0.2%).

Organ weights

The spleens of SS mice were more than 10-fold greater in weight than those of control mice when expressed as either actual organ weights or as percentages of body weights ($P < .001$). Similarly, the brains and hearts of SS mice also were significantly heavier than those of control mice even after controlling for age and sex. The liver and kidney weights in both control and SS mice were strongly positively associated with both male sex and increasing age; after controlling for these variables, there was no significant difference in these organ weights between SS and control mice.

Histopathology

The perfusion fixation was judged to be of high quality since fewer than 20% of mice showed morphologic evidence of hepatic pericentral venous pallor, which was used as an indication of cellular alterations due to agonal changes (Table 5).

Despite the effective perfusion, SS mice frequently had residual sickle erythrocytes in the visceral blood vessels, and this limited the masking of the specimens.

The major histopathologic findings of significant differences between the SS and control groups, along with their statistical

Table 4. Tissues and morphologic features graded

Tissue	Features graded
Brain	Pyknotic Purkinje cells; iron pigment
Eyes	Retinal degeneration; iron pigment; infarcts
Lungs	Infarcts; thickness of intima and media of pulmonary arteries; mononuclear infiltrates; iron pigment; hemorrhages; vascular congestion; dilated capillaries
Kidneys	Glomerular diameter; cysts and infarcts; thickness of vascular intima and media on 10 × near renal sinus; iron pigment; mononuclear infiltrates
Liver	Calcification; infarcts; iron pigment; mononuclear infiltrates; pericentral venous pallor; steatosis
Spleen	Diameter of spleen (mm); increased white pulp (hematopoietic cells); luminal diameter (ectasia) of blood vessel in the white pulp; iron pigment; infarcts
Heart	Infarcts (recent/remote); vascular wall thickness; iron pigment; thickness of left and right ventricular free walls (mm)
Pancreas	Greatest islet diameter
Bone marrow	Cellularity, erythroid hyperplasia, iron pigment
Intravascular erythrocytes	Percentage of cells demonstrating sickle morphology
Carotid arteries	Abnormalities of the endothelium, intima, media, and adventitia

Table 5. Pathologic findings in control and SS mice

	Genotype		
	Control; n = 16	Sickle; n = 15	*P*
Spleen			
Gross infarcts, % positive	0	27	.04
Micros infarct, % positive	0	40	.007
Diameter, mm	2.2	5.7	< .001
Iron, all ages	1.9	4.4	< .001
2 y or younger	0	2.7	NA
Older than 2 y	2.6	5.9	NA
Hematopoiesis	0.3; n = 6	5.9	< .001
Vascular ectasia, all ages	0.8	4.4	< .001
2 y or younger	0.5	3.7	NA
Older than 2 y	0.9	5.0	NA
Liver			
Mononuclear, % positive	6	67	< .001
Gross infarcts, % positive	0	27	.04
Micros infarcts, % positive	0; n = 6	100	< .001
Iron, % positive	0	100	< .001
Iron, mean of positive scores	NA	4.1	NA
Calcification, % positive	0	60	< .001
Perivenous pallor, % positive	6	20	NS
Kidney			
Cortical width, μm	25.8	42.1	< .001
Gross infarcts, % positive	0	20	.10
Micros infarcts, % positive	0	67	< .001
Iron, % positive*	6	93	< .001
Iron, mean of positive scores	1.0	4.1	NA
Glomerular size, U	2.7	4.5	< .001
Arterial wall, μm	1.7	2.1	NS
Mononuclear infiltrates, % positive	0	40	.007
Lungs			
Lymphs, % positive	12.5	20	NS
Iron, all ages, % positive	0	80	< .001
2 y or younger	0	57	NA
Older than 2 y	0	100	NA
Iron, all ages, mean of positive scores	NA	1.75	NA
Capillary congestion, % positive	0; n = 6	93	.001
Pulmonary artery wall, μm	1.8	2.7	.002
Hemorrhage, % positive	0; n = 6	60	.02
Heart			
Micros infarcts, % positive	0	33	.02
Iron, % positive	6	33	.08
Iron, mean of positive scores	1.0	1.2	NA
Blood vessel diameter, μm†	3.7; n = 15	4.9	.02
Blood vessel wall thickness, % greater than 1 μm	12.5	80	< .001
Brain and eye			
Pyknotic Purkinje cells, %	0	93	< .001
Retinal degeneration, %	0	100	< .001
Bone marrow			
Iron, %	17	67	.02
Iron, mean of positive scores	1.5	1.3	NA
Cellularity score	5.1	4.2	< .001
Erythroid hyperplasia score	0.88	4.8	< .001

Measurements are mean values of all grading scores unless otherwise designated as percentage of animals with positive scores and corresponding mean of the positive scores.

NA indicates not applicable; NS, not significant.

*Among SS animals, iron scores in the kidney increased by .85 for each month of age ($P < .001$).

†Among SS animals, sex and age were independent factors associated with cardiac vascular ectasia (coefficient = 1.5 for male sex [$P = .03$] and .44 for each month of age [$P = .03$]).

significance, are shown in Table 5, and representative sections of spleen, bone marrow, liver, and heart are shown in Figure 1. Representative sections of lung, kidney, glomerulus, and cerebellum are shown in Figure 2.

In brief, the spleens of SS mice demonstrated splenomegaly (with maximum splenic diameter achieved in 2-3 months), expansion of splenic hematopoiesis, splenic infarcts, progressive iron deposition with age, and age-related vascular ectasia. Sections of bone marrow from vertebrae, sternums, and ribs of SS mice demonstrated somewhat less overall cellularity, thinner boney trabeculae, more clumping of hematopoietic cells, and marked erythroid hyperplasia when compared with the controls. The livers of SS mice demonstrated mononuclear-cell infiltration, both gross and microscopic infarcts, iron deposition, and calcifications, but no steatosis. The hearts of SS animals demonstrated increased diameters of blood vessels, microscopic infarcts, and increased iron deposition. The lungs of SS mice demonstrated hemorrhage, progressive iron deposition, capillary congestion, and increased wall thickness of pulmonary arteries. The kidneys of SS mice demonstrated increased cortical width, both gross and microscopic infarcts, iron deposition, enlarged glomeruli with the appearance of increased mesangium, and mononuclear-cell infiltration. In the cerebellum of more than 90% of SS

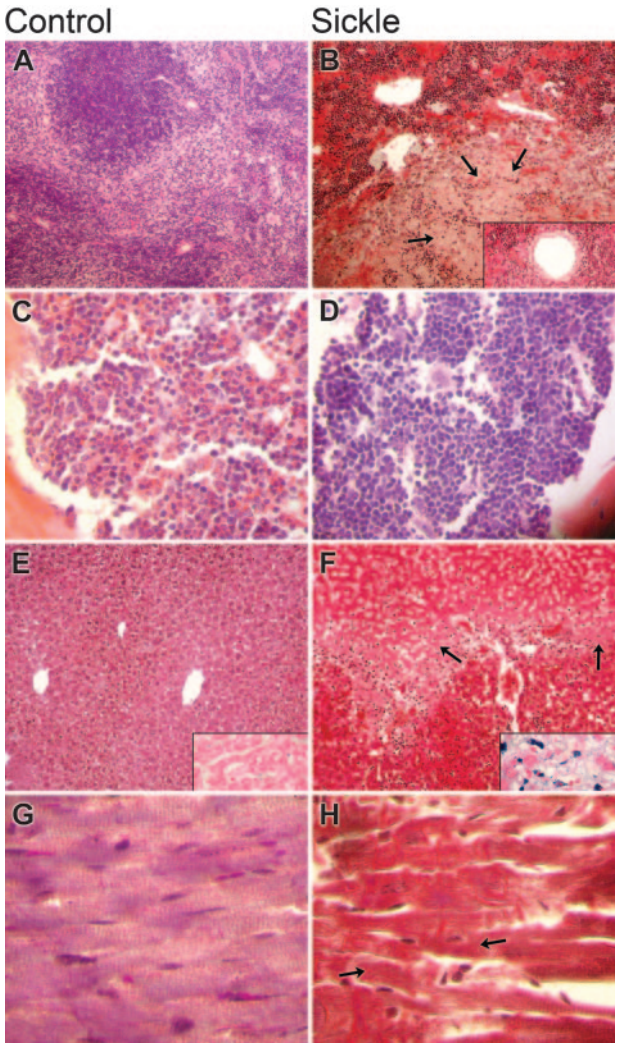

Figure 1. Comparison of histopathology in control and sickle mice. The columns show microscopic findings in control (A, C, E, G) and sickle (B, D, F, H) mice. The 4 rows (top to bottom) show findings in the spleen (A, B), bone marrow (C, D), liver (E, F), and heart (G, H). (A, B) Sickle mice had severe splenic sinusoidal congestion by sickle erythrocytes, increased hematopoietic cells, infarcts (arrows), and vascular ectasia (inset) (H&E original magnification, 100 ×; inset, 400 ×). (C, D) Erythroid hyperplasia was more severe in the bone marrow of sickle mice (H&E original magnification, 100 ×). (E, F) Hepatic findings in sickle mice included more sinusoidal congestion, infarct, and siderosis (inset) (H&E original magnification, 100 ×; insets iron stain, 400 ×). (G, H) Cardiac findings in sickle mice included infarcts, which, when acute, appeared as loss of normal striations (arrows).

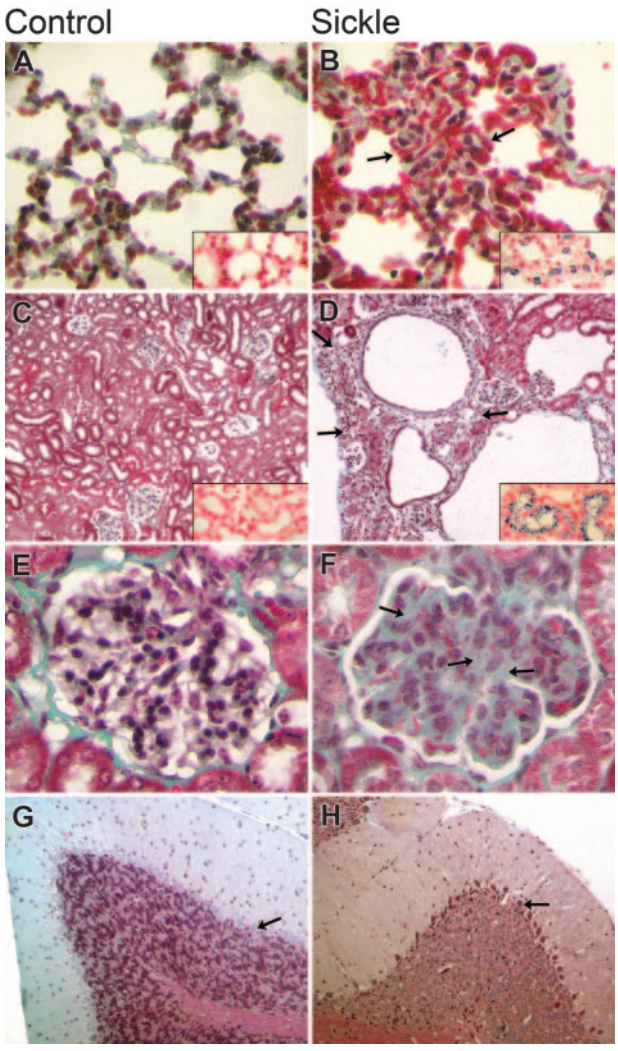

Figure 2. Comparison of histopathology in control and sickle mice. The columns show microscopic findings in control (A, C, E, G) and sickle (B, D, F, H) mice. The 4 rows (top to bottom) show findings in the lung (A, B), kidney (C, D), glomerulus (E, F), and cerebellum (G, H). (A, B) Pulmonary findings in the sickle mice included more severe vascular congestion (arrows) and siderosis (inset) (H&E original magnification, 100 ×; inset iron stain, 100 ×). (C, D) Renal findings included infarcts (arrows) and siderosis (inset) in the sickle mice (Trichrome stain original magnification, 100 ×; inset iron stain, 100 ×). (E, F) Glomerular changes in the sickle mice included mesangial hyperplasia (arrows). (Trichrome stain original magnification, 400 ×). (G, H) Cerebellar findings included pyknotic Purkinje cell in the sickle mice (arrows) (Trichrome stain original magnification, 100 ×).

mice, Purkinje cells were frequently pyknotic, but no pyknotic Purkinje cells were present in the controls.

Scanning electron microscopic analysis of control mouse cerebral vessels perfused with the fluorescent plasma marker FITC-dextran demonstrated normal-sized and normally perfused microvessels (Figure 3A).

The SS mouse, however, exhibited irregularly dilated cerebral microvessels with diffuse extravascular leakage of FITC-dextran ($n = 2$; Figure 3B,C), indicating abnormal vascular permeability.

SS mice between the ages of 1 and 6 months also were notable for not having many of the histologic findings that have been described in humans of variable ages with sickle cell disease, including bone marrow infarcts, splenic atrophy, sickle retinopathy, intimal thickening within systemic vasculature, pulmonary vascular plexiform lesions, pulmonary fat or bone marrow emboli, thromboemboli, renal papillary necrosis, pulmonary infarcts, or disruption of vascular elastic lamina. Moreover, no significant pathologic changes were identified in sections of carotid arteries, cortical bone, pancreas, stomach, small intestines, large intestines, or thymus.

The only histopathologic feature that showed an association with sex was the measurement of cardiac vascular diameters, which was significantly greater in male than in female SS mice. Significant associations with age were observed for ectasia of cardiac vascular diameters and siderosis in the kidneys and, using 2 months of age as the cutoff, with ectasia of splenic arteries and siderosis in spleen and lungs (Table 5).

SS mice had extremely thin retinas with only a single layer of variably attenuated retinal blood vessels and pigmented lesions (Figure 4B).

With bright-field illumination, it was apparent that the pigmented lesions were associated with the remaining retinal vasculature (Figure 4D). Sectioning of these retinas demonstrated that there was no outer nuclear layer (photoreceptors), and the pigmented lesions were retinal pigment epithelial cells (RPEs) that had migrated into the retina and ensheathed surviving blood vessels. The histopathology suggested that the retinal degeneration in SS mice might be due to homozygous mutations in a retinal phosphodiesterase gene (rd1 mutation) ($Pde6b^{rd1}$), which has previously been described in one of the Berkeley parental strains (FVB).[9,10] This hypothesis was confirmed by analysis of genomic DNA, which demonstrated homozygous rd1 mutations in the SS mice with retinal lesions. Hemizygous mice also had retinal degeneration, and these also were homozygous for the rd1 mutation.

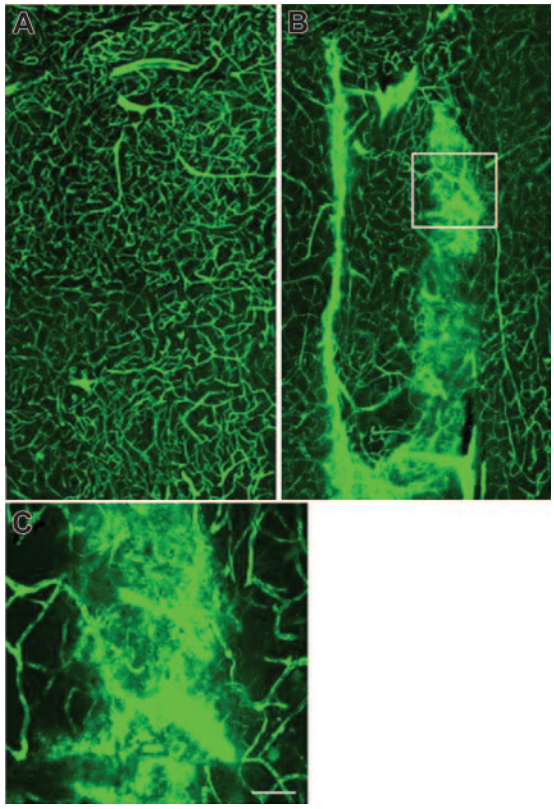

Figure 3. Cerebral microvessels perfused with FITC-dextran. The plasma-demarcated capillary networks show a broad array of twists, turns, and junctions in the striatum from a control mouse (A). Irregularly dilated cerebral microvessels with leakage of FITC-dextran was detected in the striatum of an SS mouse (B, C). Panel C is a high magnification of boxed area in panel B (Bar = 40 μm).

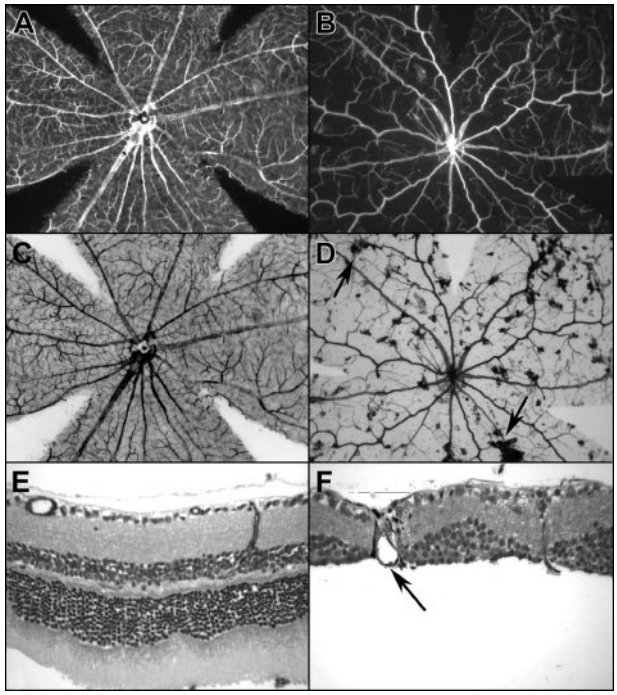

Figure 4. Retinas from 1-year-old Berkeley SS mice that were heterozygous or homozygous for the rd1 mutation. (A, C, E) Heterozygous for the rd1 mutation; (B, D, F) homozygous for the rd1 mutation. Retinas were incubated for enzyme histochemical demonstration of ADPase activity and then flat-embedded in JB-4. The ADPase activity in viable blood vessels appears white with dark-field illumination (A, B) and black with bright-field illumination (C, D). (A) The normal mouse retina has a spoke wheel pattern of blood vessels that emanates from the optic nerve head (center). (B) The Berkeley mouse that was homozygous for rd1 had a much attenuated retinal vasculature and was missing the dense, deep capillary system. (C) There was no pigment present in the retina of the mouse heterozygous for rd1 with bright-field illumination. (D) The Berkeley rd1/rd1 mouse had many areas that were pigmented, suggesting that the retinal pigment epithelial (RPE) cells had migrated into the sensory retina (arrow). (E) When the normal-appearing retina in panels A and C was sectioned, the 2 nuclear layers of retina were apparent, and photoreceptor outer segments were present below the outer nuclear layer (bottom). The retinal vasculature in the inner retina appeared normal, and a vessel is seen connecting the superficial and deep capillary systems of the retina in this field. (F) The Berkeley rd1/rd1 mouse had no outer nuclear layer or photoreceptor outer or inner segments (bottom), a disorganized inner nuclear layer (bottom), and RPE cells (arrow) had migrated into the retina and ensheathed a dilated blood vessel.

Discussion

Berkeley SS mice demonstrate a wide spectrum of hematologic and histopathologic findings that are very similar to those found in humans with sickle cell disease, and yet there clearly are notable differences. Since even a minor difference in hematologic parameters can profoundly affect the severity of human sickle cell disease, in particular, erythrocyte MCHC and levels of fetal hemoglobin, it is important to compare the hematologic manifestation of SS mice to humans with sickle cell disease. SS mice have marked sickling, but the erythrocytes demonstrate a mild β-thalassemia phenotype, with reduced MCHC, as a result of a decreased rate of β globin synthesis relative to α globin.[2,4] Since erythrocyte sickling increases as the intraerythrocytic hemoglobin concentration increases, the reduction in MCHC in SS mice would be expected to offer some protection from erythrocyte sickling, and thus perhaps from vaso-occlusion and organ damage. Despite this, erythrocyte sickling is severe in SS mice, and erythrocyte survival is very short.[3] Moreover, in humans, HbS-β^0 thalassemia is a clinically severe form of sickle cell disease, albeit with fewer cerebral infarcts, despite its association with reduced MCHC.[11]

Humans with sickle cell disease express variable amounts of fetal hemoglobin, and higher fetal hemoglobin levels are associated with less severe manifestations of the disease. Berkeley SS mice express exceedingly low levels of hemoglobin F after birth,[2] and this low level would be expected to counterbalance some of the protection afforded by the reduced hemoglobin concentration. In fact, Fabry et al[4] produced a series of mice expressing sickle hemoglobin with nearly balanced (β^s/α) globin chain synthesis (0.93 ratio) in conjunction with 3 different levels of hemoglobin F (low, 3%; moderate, 20%; and high, 40%). The NY1KO mice with moderate (20%) hemoglobin F levels most closely resemble the Berkeley mice with regard to level of anemia, reticulocytosis, urine concentrating deficit, and severity of histopathologic findings. The NY1KO mice with very low levels of hemoglobin F had much more severe organ pathology and markedly reduced survival compared to either the Berkeley mice or the NY1KO mice with 20% hemoglobin F.[12] These data suggest that in the absence of either a thalassemic phenotype or high levels of hemoglobin F, murine mouse models of sickle cell disease exhibit greater severity of disease than humans with sickle cell disease. Thus, either a mild β thalassemic phenotype, as in the Berkeley mice, or an increased hemoglobin F level, as in the NY1KO mice, appears to be required for survival beyond several months of age.

Hemizygous Berkeley mice, which lack mouse α globin and are heterozygous for mouse β globin, segregate into 2 subpopulations containing approximately 26% and 42% hemoglobin S due to the presence of either 1 or 2 copies of the human $\alpha 1\ \gamma\ \delta\ \beta^s$ transgene, respectively.[13] Paradoxically, mice with only one copy of the transgene appear to be more sensitive to hypoxia and have more severe renal involvement than mice with 2 copies of the transgene, even though they have less hemoglobin S.[13] Noguchi et al[14] ascribed these observations to the low oxygen affinity (P_{50}) of the chimeric human α murine β hemoglobin, which is more abundantly expressed in mice with only a single transgene. We also examined the pathology of hemizygous Berkeley mice with one copy of the human transgene (data not shown). The histopathologic abnormalities in these animals were generally intermediate between those of control and sickle mice, except for the kidney, where we confirmed the severe pathology previously reported by Noguchi et al[14] and Diwan et al,[15] as well as the cerebellum, where the Purkinje-cell abnormalities of the hemizygous mice were as severe as in the SS mice (data not shown). We also found increased splenic hematopoiesis without associated enlargement of the spleens in the hemizygous mice. It is important to emphasize, however, that the phenotype derived from the combination of a high O_2 affinity hemoglobin and hemoglobin S does not correspond to a well-defined human category. Therefore, the hemizygous mice should not be considered a model of human sickle cell trait or human sickle cell disease.

Histopathologic findings in SS mice that are similar to those in human sickle cell disease include evidence of intravascular hemolytic anemia (cardiomegaly, renal tubular and hepatic reticuloendothelial siderosis, and exuberant hematopoiesis), vaso-occlusion (intravascular sickle cells, pyknotic Purkinje cells, multifocal visceral infarcts, and hemorrhages), vascular changes (pulmonary congestion and increased diameter of blood vessels in spleen and heart), pulmonary hemorrhages, siderosis (heart, lungs, kidneys, and spleen), and glomerular hypertrophy.[16]

Our findings in 1- to 6-month-old SS mice differ from those in human sickle cell disease patients of variable ages in several features. In the spleen, SS mice show splenomegaly rather than atrophy. Whereas splenomegaly in SS mice appears within the first month and is associated with markedly expanded hematopoiesis that persists into adulthood, the initial splenic hypertrophy in

human sickle cell disease (until about 2 years of age) is usually followed by progressive siderofibrosis and atrophy with virtual asplenia in adulthood.[17,18] Although both murine and human sickle cell disease feature exuberant hematopoiesis, the sites of the hematopoiesis differ. In sickle mice the spleen is the primary hematopoietic organ, which expands to accommodate the increased demand. In human sickle cell disease the bone marrow is the primary hematopoietic organ and is more limited in its capacity for expansion within its compartment of bone, making the marrow more susceptible to compression and ischemic injury. Additionally, in human sickle cell disease, marrow expansion occurs in nonhematopoietic fatty marrow,[4] which then cannot only become the site of infection, infarction, and/or bone marrow embolism, but may also weaken the bone, predisposing it to pathologic fracture.[19,20]

Previous studies have shown similarities in the severity of renal structural and functional changes in SS mice compared with humans with sickle cell disease, including early nephromegaly, glomerular hypertrophy, cortical fibrosis with cyst formation, chronic interstitial nephritis, renal tubular siderosis, and concentrating defects.[4,21-25] Further studies will be required to establish whether the glomerular lesions are identical to the mesangioproliferative glomerulopathy found in sickle cell disease patients. In this study, several important dissimilarities were noted, including the absence of papillary necrosis and more severe injury to the renal cortex in SS mice than in humans with sickle cell disease.

Hepatic pathology in SS mice is similar to that in humans with sickle cell disease with regard to congestion, siderosis, infarcts, and hepatomegaly.[4] SS mice are dissimilar in having calcifications and a greater number of, and larger, infarcts. In addition the SS mice do not have viral-like hepatitis, or cholestasis, which are relatively common in human sickle cell disease.[26-28]

Cardiac pathology in SS mice is similar to that in humans with sickle cell disease with regard to cardiomegaly and infarcts in the absence of major coronary artery disease, suggesting vaso-occlusion of the small intracardiac vessels contributes to the pathogenesis of the ischemic injury.[29-31]

Pulmonary pathology in SS mice is similar to that in humans with sickle cell disease in intravascular sickle cell congestion, hemorrhages, siderosis, and pulmonary medial hypertrophy, but dissimilar in showing much less severe inflammatory and ischemic changes, with no evidence of pneumonia, vascular intimal hyperplasia, plexiform lesions, thromboemboli, fat or bone marrow emboli, edema, interstitial pneumonitis, mucous plugs, or infarcts.[32-34] The marked intravascular sickle cell congestion that we observed may be due to the increased expression of endothelial-cell adhesion molecules in the lungs of Berkeley sickle cell mice reported previously by Belcher et al.[35]

Systemic vascular pathology in these relatively young SS mice is similar to that in young humans with sickle cell disease in showing congestion of small vessels by sickle cells and ectasia, but dissimilar in showing no significant intimal or medial hyperplasia, mural thrombi, perivascular fibrosis, or abnormalities of the elastic lamina (Figure 4D).[36-38]

Central nervous system pathology in SS mice is similar to that in humans with sickle cell disease in showing evidence of ischemic injury. These ischemic changes in the mice were pyknotic neurons (Purkinje cells) but in humans are reported as clinically apparent or silent strokes.[11] The findings are also dissimilar in showing no large vessel vasculopathy, thrombotic/embolic infarcts, or hemorrhagic strokes.[39-43] It is particularly striking that no cerebral infarctions were seen, because such infarcts occur in children with sickle cell disease.[37-39] The circle of Willis is frequently the site of vascular abnormalities in children with stroke, and thus it is possible that the unusual rheologic characteristics of the circle of Willis contribute to the development of large vessel disease.[40] The circle of Willis is variably developed in mice, depending on the genetic background, and while this might be expected to enhance the likelihood of stroke because of reduced collateral circulation, it also may affect rheologic factors that make the cerebral circulation vulnerable to stenosis and thrombosis in humans with sickle cell disease.

Pathology of the bone marrow in SS mice is similar to that in humans with sickle cell disease in demonstrating erythroid hyperplasia and thinning of boney trabeculae, but dissimilar in the absence of thrombosis, perivascular fibrosis, osteomyelitis, or infarcts.[18,38,44]

Finally, SS mice differ from humans with sickle cell disease in showing early rapid retinal degeneration with nearly complete loss of the outer retinal layers, rather than the retinopathy typical of humans with sickle cell disease.[45-49] This was a striking incidental finding, which also has been reported in the FVB mouse strain (one of the parental strains of the Berkeley SS mouse) and is most likely caused by the homozygous mutation we identified in a retinal phosphodiesterase gene (rd1 genotype, PDEGF; 180072; 4p16.3).[8,9,10] In unpublished studies by one of us (G.A.L., August 2005), approximately 25% of SS mice and 50% of hemizygous mice derived from another subcolony of Berkeley mice did not demonstrate retinal degeneration; these mice were heterozygous for the rd1 mutation. Thus, by chance, our subcolony appears to have developed a higher frequency of the rd1 mutation.

Overall, our findings demonstrate that the Berkeley SS mouse is likely to be a good model of human sickle cell disease for studies of chronic hemolytic anemia; small-vessel vaso-occlusion by sickle cells; chronic tissue hypoxia of heart, liver, kidneys, and brain; increased hematopoiesis; vascular ectasia; and sickle nephropathy. It is perhaps less well suited for studies of chronic sickle lung disease, the vasculopathy typical in humans with sickle cell disease, bone marrow infarcts, bone marrow or fat pulmonary emboli, retinopathy, renal papillary necrosis, and splenic atrophy.

We conclude that Berkeley SS mice have marked similarities to humans with sickle cell disease in many, but not all, organs. The differences, which probably reflect fundamental differences in hematopoiesis and organ physiology between the species, warrant careful consideration when using the Berkeley SS mouse as a model for human sickle cell disease.

Acknowledgments

We would like to acknowledge Sandra Holzhauer and Terri Besch for their expert technical assistance with the mouse perfusions and phlebotomy; Weiming Yang for the polymerase chain reaction analysis of rd1; and Suzanne Rivera for outstanding secretarial assistance.

References

1. Paszty C. Transgenic and gene knock-out mouse models of sickle cell anemia and the thalassemias. Curr Opin Hematol. 1997;4:88-93.
2. Paszty C, Brion CM, Manci E, et al. Transgenic knockout mice with exclusively human sickle hemoglobin and sickle cell disease. Science. 1997; 278:876-878.
3. de Jong K, Emerson RK, Butler J, Bastacky J, Mohandas N, Kuypers FA. Short survival of phosphatidylserine-exposing red blood cells in murine sickle cell anemia. Blood. 2001;98: 1577-1584.
4. Fabry ME, Suzuka SM, Weinberg RS, et al. Second generation knockout sickle mice: the effect of HbF. Blood. 2001;97:410-418.

5. Kean LS, Manci EA, Perry J, et al. Chimerism and cure: hematologic and pathologic correction of murine sickle cell disease. Blood. 2003;102: 4582-4593.
6. Lutty GA, McLeod DS. A new technique for visualization of the human retinal vasculature. Arch Ophthalmol. 1992;110:267-276.
7. Zhang Z, Davies K, Prostak J, Fenstermacher J, Chopp M. Quantitation of microvascular plasma perfusion and neuronal microtubule-associated protein in ischemic mouse brain by laser-scanning confocal microscopy. J Cereb Blood Flow Metab. 1999;19:68-78.
8. Pittler SJ, Baehr W. Identification of a nonsense mutation in the rod photoreceptor cGMP phosphodiesterase beta-subunit gene of the rd mouse. Proc Natl Acad Sci U S A. 1991;88:8322-8326.
9. Carter-Dawson LD, LaVail MM, Sidman RL. Differential effect of the rd mutation on rods and cones in the mouse retina. Invest Ophthalmol Vis Sci. 1978;17:489-498.
10. Chang B, Hawes NL, Hurd RE, Davisson MT, Nusinowitz S, Heckenlively JR. Retinal degeneration mutants in the mouse. Vision Res. 2002;42: 517-525.
11. Driscoll MC, Hurlet A, Styles L, et al. Stroke risk in siblings with sickle cell anemia. Blood. 2003;101: 2401-2404.
12. Fabry ME, Suzuka SM, Aggarwal S, Nagel RL. Unexpected impact of HbF on mean survival time of BERK sickle transgenic mice expressing exclusively human hemoglobins [abstract]. Blood. 2002;100:2617a.
13. Noguchi CT, Gladwin MT, Diwan B, et al. Developing a useful model for sickle cell disease: hemizygotes for the mouse beta-globin gene [abstract]. Blood. 2000;96:598a.
14. Noguchi CT, Gladwin M, Diwan B, et al. Pathophysiology of a sickle cell trait mouse model: human alpha(beta)(S) transgenes with one mouse beta-globin allele. Blood Cells Mol Dis. 2001;27: 971-977.
15. Diwan BA, Gladwin MT, Noguchi CT, Ward JM, Fitzhugh AL, Buzard GS. Renal pathology in hemizygous sickle cell mice. Toxicol Pathol. 2002;30:254-262.
16. Song J. Pathology of Sickle Cell Disease. Springfield, IL: Charles C. Thomas; 1971.
17. Rogers DW, Vaidya S, Serjeant GR. Early splenomegaly in homozygous sickle-cell disease: an indicator of susceptibility to infection. Lancet. 1978;2:963-965.
18. Stevens MC, Hayes RJ, Vaidya S, Serjeant GR. Fetal hemoglobin and clinical severity of homozygous sickle cell disease in early childhood. J Pediatr. 1981;98:37-41.
19. Mankad VN, Yang YM, Williams JP, Brogdon BG. Magnetic resonance imaging of bone marrow in sickle cell patients. Am J Pediatr Hematol Oncol. 1988;10:344-347.
20. Keeley K, Buchanan GR. Acute infarction of long bones in children with sickle cell anemia. J Pediatr. 1982;101:170-175.
21. Morgan AG, Shah DJ, Williams W. Renal pathology in adults over 40 with sickle-cell disease. West Indian Med J. 1987;36:241-250.
22. Pitcock JA, Muirhead EE, Hatch FE, Johnson JG, Kelly BJ. Early renal changes in sickle cell anemia. Arch Pathol. 1970;90:403-410.
23. Walker BR, Alexander F, Birdsall TR, Warren RL. Glomerular lesions in sickle cell nephropathy. JAMA. 1971;215:437-440.
24. Tejani A, Phadke K, Adamson O, Nicastri A, Chen CK, Sen D. Renal lesions in sickle cell nephropathy in children. Nephron. 1985;39:352-355.
25. Verani RR, Conley SB. Sickle cell glomerulopathy with focal segmental glomerulosclerosis. Child Nephrol Urol. 1991;11:206-208.
26. Omata M, Johnson CS, Tong M, Tatter D. Pathological spectrum of liver diseases in sickle cell disease. Dig Dis Sci. 1986;31:247-256.
27. Mills LR, Mwakyusa D, Milner PF. Histopathologic features of liver biopsy specimens in sickle cell disease. Arch Pathol Lab Med. 1988;112:290-294.
28. Bauer TW, Moore GW, Hutchins GM. The liver in sickle cell disease: a clinicopathologic study of 70 patients. Am J Med. 1980;69:833-837.
29. Gerry JL, Bulkley BH, Hutchins GM. Clinicopathologic analysis of cardiac dysfunction in 52 patients with sickle cell anemia. Am J Cardiol. 1978; 42:211-216.
30. Hardison JE, Rogers CM. Cardiovascular manifestations of sickle cell anemia. In: Hurst JW, ed. The Heart. New York, NY: McGraw-Hill; 1979: 195.
31. Martin CR, Johnson CS, Cobb C, Tatter D, Haywood LJ. Myocardial infarction in sickle cell disease. J Natl Med Assoc. 1996;88:428-432.
32. Vichinsky EP, Styles LA, Colangelo LH, Wright EC, Castro O, Nickerson B. Acute chest syndrome in sickle cell disease: clinical presentation and course: Cooperative Study of Sickle Cell Disease. Blood. 1997;89:1787-1792.
33. Vichinsky EP, Neumayr LD, Earles AN, et al. Causes and outcomes of the acute chest syndrome in sickle cell disease: National Acute Chest Syndrome Study Group. N Engl J Med. 2000;342:1855-1865.
34. Haupt HM, Moore GW, Bauer TW, Hutchins GM. The lung in sickle cell disease. Chest. 1982;81: 332-337.
35. Belcher JD, Bryant CJ, Nguyen J, et al. Transgenic sickle mice have vascular inflammation. Blood. 2003;101:3953-3959.
36. Merkel KH, Ginsberg PL, Parker JC Jr, Post MJ. Cerebrovascular disease in sickle cell anemia: a clinical, pathological and radiological correlation. Stroke. 1978;9:45-52.
37. Tuohy AM, McKie V, Manci EA, Adams RJ. Internal carotid artery occlusion in a child with sickle cell disease: case report and immunohistochemical study. J Pediatr Hematol Oncol. 1997;19:455-458.
38. Manci EA, Culberson DE, Gardner JM, et al. Perivascular fibrosis in the bone marrow in sickle cell disease. Arch Pathol Lab Med. 2004;128: 634-639.
39. Baird R, Weiss D, Ferguson A, French J, Scott R. Studies in sickle cell anemia, XXI: clinicopathological aspects of neurological manifestations. Pediatrics. 1964;34:92-100.
40. Ohene-Frempong K, Weiner SJ, Sleeper LA, et al. Cerebrovascular accidents in sickle cell disease: rates and risk factors. Blood. 1998;91:288-294.
41. Rothman S, Nelson JS. Stenosis of large caliber intracranial arteries and cerebral infarctions in sickle cell anaemia. Lab Invest. 1978;38:392.
42. Stockman JA, Nigro MA, Mishkin MM, Oski FA. Occlusion of large cerebral vessels in sickle-cell anemia. N Engl J Med. 1972;287:846-849.
43. Koshy M, Thomas C, Goodwin J. Vascular lesions in the central nervous system in sickle cell disease (neuropathology). J Assoc Acad Minor Phys. 1990;1:71-78.
44. Mankad VN, Williams JP, Harpen MD, et al. Magnetic resonance imaging of bone marrow in sickle cell disease: clinical, hematologic, and pathologic correlations. Blood. 1990;75:274-283.
45. Rothman SM, Fulling KH, Nelson JS. Sickle cell anemia and central nervous system infarction: a neuropathological study. Ann Neurol. 1986;20: 684-690.
46. Adams RJ, McKie VC, Hsu L, et al. Prevention of a first stroke by transfusions in children with sickle cell anemia and abnormal results on transcranial Doppler ultrasonography. N Engl J Med. 1998;339:5-11.
47. Romayanada N, Goldberg MF, Green WR. Histopathology of sickle cell retinopathy. Trans Am Acad Ophthalmol Otolaryngol. 1973;77:OP642-OP676.
48. Welch RB, Goldberg MF. Sickle-cell hemoglobin and its relation to fundus abnormality. Arch Ophthalmol. 1966;75:353-362.
49. Asdourian G, Nagpal KC, Goldbaum M, Patrianakos D, Goldberg MF, Rabb M. Evolution of the retinal black sunburst in sickling haemoglobinopathies. Br J Ophthalmol. 1975;59:710-716.

2006 107: 1651-1658
doi:10.1182/blood-2005-07-2839 originally published online
September 15, 2005

Pathology of Berkeley sickle cell mice: similarities and differences with human sickle cell disease

Elizabeth A. Manci, Cheryl A. Hillery, Carol A. Bodian, Zheng G. Zhang, Gerard A. Lutty and Barry S. Coller

Blood (print ISSN 0006-4971, online ISSN 1528-0020), is published weekly by the American Society of Hematology, 2021 L St, NW, Suite 900, Washington DC 20036.